Molecular Biology of the Cell
Vol. 19, 3735–3744, September 2008

# Anillin-mediated Targeting of Peanut to Pseudocleavage Furrows Is Regulated by the GTPase Ran

**Rosalind V. Silverman-Gavrila,*† Karen G. Hales,‡§ and Andrew Wilde***

*Department of Molecular Genetics, University of Toronto, M5S 1A8 Toronto, ON, Canada; and ‡Department of Biology, University of North Carolina at Chapel Hill, Chapel Hill, NC 27599-3280

Submitted January 18, 2008; Revised June 6, 2008; Accepted June 16, 2008
Monitoring Editor: Yu-Li Wang

**During early development in *Drosophila*, pseudocleavage furrows in the syncytial embryo prevent contact between neighboring spindles, thereby ensuring proper chromosome segregation. Here we demonstrate that the GTPase Ran regulates pseudocleavage furrow organization. Ran can exert control on pseudocleavage furrows independently of its role in regulating the microtubule cytoskeleton. Disruption of the Ran pathway prevented pseudocleavage furrow formation and restricted the depth and duration of furrow ingression of those pseudocleavage furrows that did form. We found that Ran was required for the localization of the septin Peanut to the pseudocleavage furrow, but not anillin or actin. Biochemical assays revealed that the direct binding of the nuclear transport receptors importin $\alpha$ and $\beta$ to anillin prevented the binding of Peanut to anillin. Furthermore, RanGTP reversed the inhibitory action of importin $\alpha$ and $\beta$. On expression of a mutant form of anillin that lacked an importin $\alpha$ and $\beta$ binding site, inhibition of Ran no longer restricted the depth and duration of furrow ingression in those pseudocleavage furrows that formed. These data suggest that anillin and Peanut are involved in pseudocleavage furrow ingression in syncytial embryos and that this process is regulated by Ran.**

## INTRODUCTION

During cytokinesis, the ingressing plasma membrane physically divides the mother cell into two daughter cells (Glotzer, 2001). Membrane ingression during cell division is both temporally and spatially regulated, ensuring that membrane scission occurs 1) only after the chromosomes have fully segregated and 2) between the two chromosomal masses. The signals within the cell that determine cytokinetic furrow positioning are complex, reflecting the strict control needed to ensure that cytokinesis is successful. Signals from astral microtubules (D'Avino *et al.*, 2005), the spindle midbody (D'Avino *et al.*, 2005), the nucleus (Rappaport, 1991), and the membrane itself (Janetopoulos and Devreotes, 2006) direct the assembly of the contractile ring to the equatorial cortex of the plasma membrane (Glotzer, 2001; Eggert *et al.*, 2006). The contractile ring is an actomyosin-based structure that constricts and generates the force needed to drive membrane ingression. As the membrane ingresses, it is remodeled and stabilized (Albertson *et al.*, 2005).

Other membrane ingression events share many of the same features and involve many of the same proteins as cytokinetic furrows. In the syncytial *Drosophila* embryo before cellularization, up to 6000 closely packed nuclei exist in a common cytosol close to the cortex. To ensure faithful chromosome segregation during the rapid nuclear divisions, nuclei are isolated from one another to prevent neighboring spindles from contacting and fusing (Sullivan *et al.*, 1990). To achieve this, plasma membrane ingressions form transiently between nuclei during the rapid nuclear cycles before cellularization (Warn *et al.*, 1984). These membrane ingressions, termed pseudocleavage or metaphase furrows, are organized by the actin cytoskeleton (Callaini *et al.*, 1992) and bear a close resemblance to cytokinetic cleavage furrows (Mazumdar and Mazumdar, 2002). First actin caps form at the plasma membrane above each nucleus. Then during interphase, as the centrosomes migrate to either side of the nucleus, the actin caps expand correspondingly. In prophase the cap reorganizes to drive membrane ingression into the embryo such that nuclei and newly forming spindles are separated from one another (Warn *et al.*, 1984). Toward the end of metaphase, the furrows begin to retract and dissipate by anaphase. This process is repeated from the tenth through the thirteenth nuclear cycles. During the fourteenth nuclear cycle, the syncytial embryo cellularizes to form 6000 columnar epithelial cells. In this instance the cleavage furrows extend down into the embryo, before growing transversally and fusing to form a single layer of nucleated cells (Foe and Alberts, 1983).

Most components required for furrow ingression are conserved between cytokinetic furrows and pseudocleavage furrows (Mazumdar and Mazumdar, 2002). However, there are some differences. Notably pseudocleavage furrows are membrane ingressions that do not meet and therefore do not lead to membrane fusion. Instead they extend into the embryo, perpendicular to the cortex, and then retract back toward the embryo cortex after the chromosomes have begun to segregate. In addition, there is a difference in the stage of the cell cycle when the furrow components assem-

This article was published online ahead of print in *MBC in Press* (http://www.molbiolcell.org/cgi/doi/10.1091/mbc.E08–01–0049) on June 25, 2008.

Present addresses: † Division of Cell and Molecular Biology, Toronto General Research Institute; § Department of Biology, Davidson College, Davidson, NC 28035.

Address correspondence to: Andrew Wilde (andrew.wilde@utoronto.ca).

Abbreviations used: MT, microtubule; NLS, nuclear localization sequence; NTR, nuclear transport receptor; SAF, spindle assembly factor.

ble. Although the cytokinetic furrow begins to assemble during anaphase and is required to divide a cell in two, the syncytial embryo pseudocleavage furrows begin to assemble in prophase and serve to prevent neighboring spindles from contacting one another (Sullivan *et al.*, 1990).

A key protein involved in cytokinetic furrow function is anillin, which has multiple domains allowing it to bind and bundle actin filaments (Field and Alberts, 1995), target septins to the plasma membrane (Oegema *et al.*, 2000; Kinoshita *et al.*, 2002), and interact with components of the microtubule-bound centralspindilin complex (Gregory *et al.*, 2008). Consequently anillin is thought to act as a scaffold for the correct assembly of the contractile ring (Piekny and Glotzer, 2007). It is not fully understood how the role of anillin in cytokinesis is regulated. However, its role in remodeling the actomyosin contractile ring in somatic cells is in part regulated by its differential spatial positioning in the cell during the cell cycle. In interphase anillin localizes to the nucleus where it cannot interact with actin and myosin at the plasma membrane. However, in mitosis upon nuclear envelope breakdown, anillin is released from the nucleus and is targeted to the cortex of the plasma membrane and later to the equatorial cortex of the plasma membrane in a RhoGTP-dependent manner (Oegema *et al.*, 2000; Piekny and Glotzer, 2007; Hickson and O'Farrell, 2008). The spatial regulation of anillin during the cell cycle contributes to the restriction of its function to mitosis. However, in *Drosophila* syncytial embryos anillin is cytosolic, localizing to pseudocleavage furrows throughout the nuclear cycle, suggesting that it may be regulated by other mechanisms.

One function of anillin is to target septins to the contractile ring (Oegema *et al.*, 2000). Septins are a family of GTP-binding proteins that can assemble into filaments (Field *et al.*, 1996). Septins have been attributed multiple roles: as membrane diffusion barriers (Takizawa *et al.*, 2000), as stabilizers of the furrow (Field *et al.*, 2005), in membrane trafficking (Albertson *et al.*, 2005), and as a scaffold (Joo *et al.*, 2007). In *Drosophila* there are five septins: Peanut, Sep1, Sep2, Sep4, and Sep5 (Neufeld and Rubin, 1994; Fares *et al.*, 1995; Field *et al.*, 1996; Adam *et al.*, 2000). Peanut, Sep1 and Sep2 have been isolated as a stoichiometric complex that in vitro can polymerize into filaments (Field *et al.*, 1996). In contrast, *Xenopus laevis* Sept2 can self assemble into filaments (Mendoza *et al.*, 2002), suggesting that septins may function independently.

The GTPase Ran is a key positive regulator of mitosis (Ciciarello *et al.*, 2007). RanGTP regulates a number of mitotic factors that are sequestered in the nucleus by nuclear transport receptors during interphase. In mitosis RanGTP antagonizes the binding of nuclear transport receptors to these proteins and thereby promotes their activity (Trieselmann *et al.*, 2003; Ems-McClung *et al.*, 2004). RanGTP is at its highest concentration around the chromosomes (Li and Zheng, 2004; Caudron *et al.*, 2005; Kalab *et al.*, 2006), where RCC1 the nucleotide exchange factor for Ran is localized. Consequently, RanGTP has been proposed to act as a spatial cue by only activating these mitotic proteins close to the chromosomes (Caudron *et al.*, 2005; Kalab *et al.*, 2006). In so doing RanGTP is thought to specify where certain mitotic processes occur in the cell. For example, it could specify that spindle assembly only occurs around chromosomes. The full extent to which this mechanism regulates the mitotic cell is not known and continues to expand.

In this study we demonstrate a new role for Ran in regulating pseudocleavage furrow ingression, a membrane invagination process in early *Drosophila* embryos. We find that the Ran pathway regulates the interaction between anillin and the septin Peanut, thereby regulating furrow stability.

## MATERIALS AND METHODS

### *Fly Stocks and Construction of Transgenic Flies*

*Drosophila melanogaster* lines used were wild-type $w^{1118}$ and lines expressing green fluorescent protein (GFP) fused to the actin-binding domain of moesin (Kiehart *et al.*, 2000), to myosin regulatory light chain (Royou *et al.*, 2002), and to α-tubulin (Grieder *et al.*, 2000).

The Sep2-GFP genomic transgene construct was generated through three sequential ligation steps. First, the *Sep2* coding region and intron plus ~540 upstream base pairs (up to the beginning of the adjacent gene's coding sequence) were amplified from wild-type genomic DNA and cloned into pCaSpeR4 (Thummel and Pirrotta, 1992) to generate pKH18A. Second, the *Sep2* 3′UTR plus ~220 downstream base pairs were amplified and cloned into pKH18A to make pKH18B. Finally, the enhanced GFP (EGFP) cDNA was cloned into pKH18B to generate a *Sep2* genomic region with the EGFP coding region inserted just before the Sep2 stop codon. Transgenic flies were generated using standard methods (Rubin and Spradling, 1982).

The GFP-anillin transgene was constructed by using PCR to amplify the anillin cDNA and the product cloned into the gateway TOPO cloning vector, pCR8/GW/TOPO (Invitrogen, Carlsbad, CA). The cDNA was then recombined into the pUASP-adapted vector in frame with GFP (T. Murphy, Carnegie Institute of Washington). Transgenic flies were then generated using standard methods (Rubin and Spradling, 1982). To make the GFP-3A-anillin transgenic flies, lysines 997–999 were mutated to alanine in the GFP-anillin gene fusion in the plasmid pCR8/GW/TOPO using the QuickChange II site-directed mutagenesis kit (Stratagene, La Jolla, CA).

### *Protein Expression, Labeling, and Purification*

Tubulin was purified from bovine brains and labeled with rhodamine as previously described (Hyman, 1991). Recombinant alleles of Ran and Ran pathway components fused to glutathione-*S*-transferase (GST) or a 6xHis-tag were expressed in BL21 *Escherichia coli* and purified as previously described (Trieselmann *et al.*, 2003). The activity of injected proteins was tested by assessing their ability to support in vitro nuclear transport in semipermeabilized HeLa cells as described previously (Brownawell *et al.*, 2002; Trieselmann and Wilde, 2002). The C-terminal domain of anillin, amino acids 815-1201 (anillin-CT), was amplified by PCR from expressed sequence tag (EST) clone LD 27393 and cloned into pGEX6P2. The GST-C terminal anillin fusion protein was expressed and purified as described previously (Trieselmann *et al.*, 2003). Lysines 997–999 were mutated as described above.

### *Embryo Microinjection*

Embryos were collected and injected at the anterior pole of the embryo as described previously (Silverman-Gavrila and Wilde, 2006) except that in this study embryos were injected in interphase as outlined in Figure 1. The initial concentrations of the injected proteins were as follows: 16 mg/ml GST-RanT24N, 14 mg/ml importin α, and 10 mg/ml rhodamine-labeled tubulin.

### *Staining of Microinjected Embryos*

Microinjected embryos were prepared for staining as described previously (Silverman-Gavrila and Wilde, 2006). The primary antibodies used were as follows: DM1A anti-α-tubulin (Sigma, Oakville, Ontario, Canada), anti-peanut (Developmental Studies Hybridoma Bank, Iowa City, IA), anti-anillin (Field and Alberts, 1995), anti-diaphanous (Afshar *et al.*, 2000), anti-cofilin

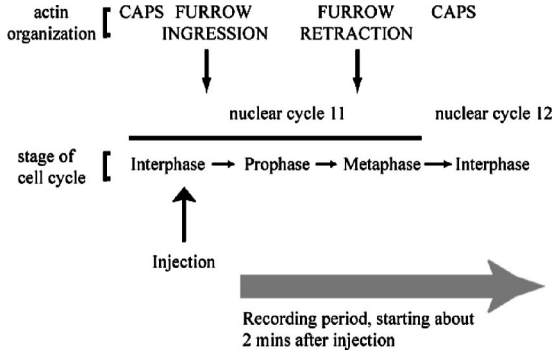


**Figure 1.** Schematic outlining the microinjection strategy used in this study. Embryos were injected during interphase and immediately imaged by time-lapse confocal microscopy.

(Niwa *et al.*, 2002), anti-Sep 2 (Adam *et al.*, 2000), and an anti-GFP (Roche, Indianapolis, IN). The secondary antibodies conjugated to Alexa488 or Alexa568 were from Molecular Probes (Eugene, OR). Actin was stained with 2 $\mu$M rhodamine phalloidin (Molecular Probes). DNA was visualized by incubating embryos with TOTO–3 iodide (Molecular Probes). The embryos were incubated with antibodies or rhodamine phalloidin overnight then washed three times for 15 min with PBS buffer containing 0.1% Triton X-100 and 0.5% BSA. Subsequently embryos were incubated with secondary antibody for 1 h and washed as described above before mounting. Each staining was performed at least three times.

### *Depolymerization of Embryonic Microtubules*

Embryos expressing GFP-tubulin were collected and prepared as described above before injection with different concentrations of colcemid to determine the minimum concentration of colcemid required to depolymerize all microtubules. At 150 $\mu$g/ml colcemid, no microtubules were observed, and we used this concentration for subsequent experiments.

### *Confocal Microscopy and Time-Lapse Imaging*

Images were captured with a Nikon Eclipse TE2000-E inverted microscope (Melville, NY) equipped with a spinning disk confocal (Perkin Elmer-Cetus Life Sciences, Boston, MA) and a Hamamatsu Orca-ER camera (Bridgewater, NJ) driven by MetaMorph software (Universal Imaging, Downingtown, PA). Images were acquired using a Plan Apochromat 40 $\times$ 1.5/NA1.0 oil immersion lens at 2–4 min after injection, in the median part of the embryo or the lateral edge of the embryo, away from the site of injection. Images were collected as a Z series of 3–5 images (40-$\mu$m steps) every 8–10 s.

### *Nuclear Trafficking Kinetics*

Embryos were collected, injected with 12 mg/ml GST-GFP-NLS and then ~10 min later were injected again with either RanT24N or buffer. Images were collected by time-lapse confocal microscopy as described above. The fluorescence intensity of GST-GFP-NLS in each nuclei in each frame of the time-lapse series of images was then determined using the region measurement feature of MetaMorph, and the background cytosolic fluorescence intensity was subtracted. The fluorescence intensity of the nuclei was then plotted over time.

### *Binding Assays*

Recombinant protein-binding assays were performed essentially as described previously (Trieselmann *et al.*, 2003). Briefly, in 200 $\mu$l of 50 mM HEPES, pH 8.0, 1 mM EGTA, 1 mM $CaCl_2$, 100 mM NaCl, different combinations of 1 $\mu$g of each protein (GST-anillin-CT, GST-3A-anillin-CT, 6xHis-RanQ69LRan, 6xHis-importin $\alpha$, or 6xHis-importin $\beta$) were incubated in the presence of glutathione agarose beads (Sigma) for 1 h at 4°C. Beads were reisolated by centrifugation, washed three times with 500 $\mu$l of 50 mM HEPES, pH 8.0, 1 mM EGTA, 1 mM $CaCl_2$, and 100 mM NaCl, and the pellets and supernatants were analyzed by SDS-PAGE and immunoblotting with an anti-His tag mouse mAb or a mouse monoclonal anti-GST antibody (Cell Signaling Technology, Beverly, MA).

Anillin-septin binding assays were carried out in a similar manner except different combinations of recombinant proteins were added to 200 $\mu$l of 0–3 h *Drosophila* embryo extract (Nelson *et al.*, 2004) in the presence of glutathione agarose beads (Sigma) for 1 h at 4°C. The beads were then collected and washed three times as described above. The pellets and supernatants were analyzed by SDS-PAGE and immunoblotted with a mouse monoclonal anti-GST antibody, or mouse monoclonal anti-peanut antibody, or an anti-Sep2 antibody.

### *Data Analysis*

To assess the effect of injections on furrow formation, we visualized furrows with an apical view of the embryo. We analyzed all furrows in the field of view in the medial region of the embryo, away from the site of injection to avoid events resulting from mechanical disruption of the embryo. Because furrows form a hexagonal array with a nucleus at the center, we defined a single furrow as that occurring between each of the vertices of the hexagon. In this context we could predict the number of furrows expected to form in the embryo based on the number of observed nuclei. To quantitate the effect of injection on furrow formation, we compared the number of furrows we observed to the number of furrows we predicted.

Furrow ingression dynamics were measured from micrographs of movies in which the lateral edges of the embryos were visualized by time-lapse spinning disk confocal microscopy. Furrow ingression dynamics were obtained by measuring the distance between the edge of the actin cap and the leading edge of the ingressing furrow at 10-s intervals. Measurements were made with the region measurement feature of MetaMorph. Furrow area was measured using Area measurement feature of MetaMorph. Statistical analysis was done with Microsoft Excel (Redmond, WA).

## RESULTS

### *The Ran Pathway Regulates Furrow Assembly and Stability*

We previously carried out a cytological screen to identify mitotic processes regulated by the Ran pathway (Silverman-Gavrila and Wilde, 2006). We injected inhibitors of the Ran pathway into GFP-$\alpha$-tubulin–expressing embryos just before mitotic entry and then monitored microtubule organization by time-lapse microscopy (Silverman-Gavrila and Wilde, 2006). One phenotype, the fusion of neighboring spindles, occurred more frequently upon the injection of inhibitors of the Ran pathway compared with control injections. In control injected embryos 0.2% of observed spindles fused to a neighboring spindle. In contrast, inhibition of the Ran pathway by injecting either the dominant negative allele of Ran, RanT24N (Kornbluth *et al.*, 1994), or importin $\alpha$ resulted in 8.4 and 7.8% of observed spindles fusing to neighboring spindles, respectively (Silverman-Gavrila and Wilde, 2006).

Because the fusion of neighboring spindles can reflect defects in pseudocleavage furrow organization (Sullivan *et al.*, 1990), we directly assessed whether perturbation of the Ran pathway affected pseudocleavage furrow organization. The actin cytoskeleton is essential for pseudocleavage furrow formation and can be used as a marker to define the pseudocleavage furrows (Callaini *et al.*, 1992). Therefore to analyze pseudocleavage furrow organization, we observed actin cytoskeleton dynamics in nuclear cycle 11 by time-lapse confocal microscopy of transgenic flies expressing GFP fused to the actin-binding domain of moesin (Kiehart *et al.*, 2000). Embryos were observed from the apical, top view of the embryo and injected during interphase when pseudocleavage furrows begin to form (Figure 1, Video 1). In control injected and uninjected embryos a hexagonal array of furrows forms around each nucleus (Figure 2A, Video 1). In contrast, upon perturbation of the Ran pathway by injection of either RanT24N or importin $\alpha$ into embryos, pseudocleavage furrows between nuclei frequently did not form and resulted in fusion of neighboring spindles (Figure 2B). To quantitate this, we compared the number of furrows we observed to the number of furrows we expected based on the assumption of a hexagonal array of pseudocleavage furrows around each nucleus. In control embryos 99.3% of the expected pseudocleavage furrows were observed (Figure 2C). In contrast, upon perturbation of the Ran pathway by injection of importin $\alpha$ or RanT24N only 75.4 or 81.5% of expected furrows were observed, respectively (Figure 2C).

In wild-type embryos, pseudocleavage furrows in nuclear cycle 11 encompassed an average area of 95.3 $\pm$ 9.7 $\mu m^2$ (n = 379) of cytoplasm around each nucleus. In contrast, the average area encompassed by pseudocleavage furrows was larger upon injection of RanT24N (109.9 $\pm$ 9.3 $\mu m^2$, n = 470, $p < 0.0001$) or importin $\alpha$ (105.8 $\pm$ 44.4 $\mu m^2$, n = 393, $p < 0.0007$). These differences were made clearer when the distribution of furrow areas was analyzed. Although control embryos had an area distribution with a single maxima, embryos injected with importin $\alpha$ or RanT24N had multiple maxima of furrow areas corresponding to furrows surrounding 1, 2, or 3 nuclei (Figure 2D). These data further confirm that furrows between nuclei were not forming.

To analyze changes in the dynamics of pseudocleavage furrow ingression into the embryo, which occurs perpendicular to the cortex, we used a focal plane deeper in the embryo (Figure 3). This analysis was performed in nuclear cycle 11, when complete ingression of individual furrows can be visualized in a single plane without interference from

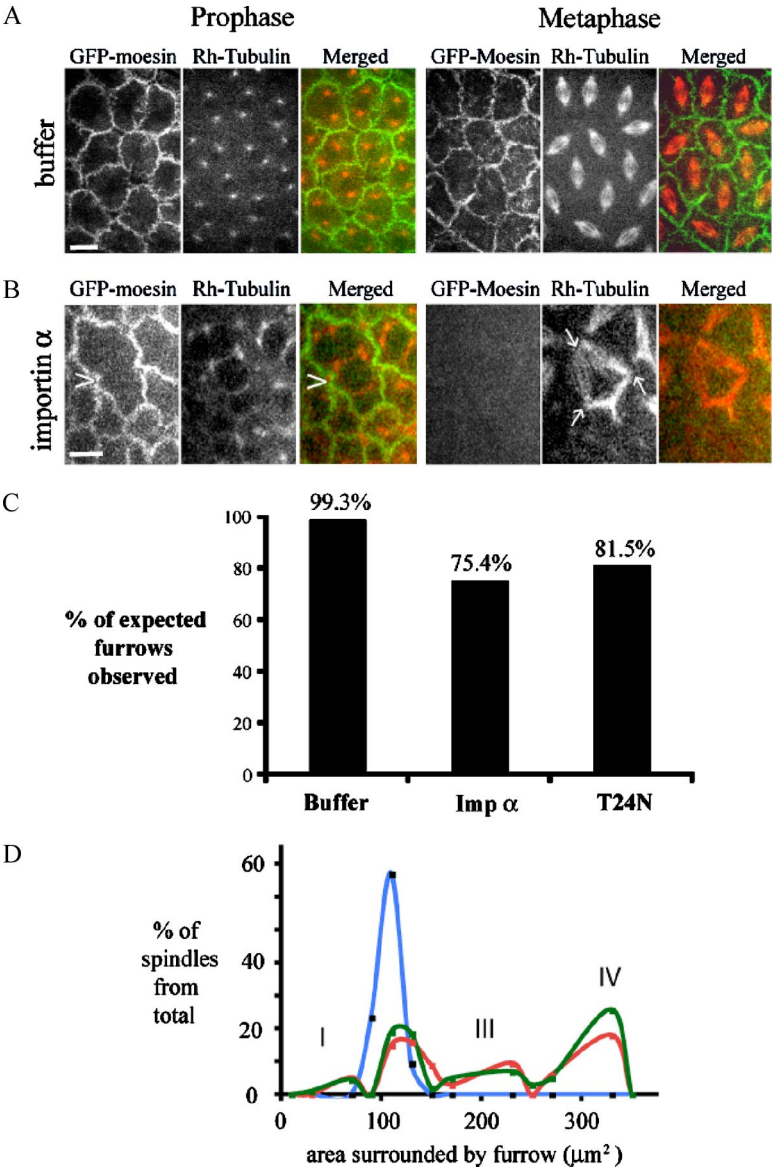


**Figure 2.** The Ran pathway is required for pseudocleavage furrow organization. (A) Micrographs from single time-lapse series showing the organization of the actin and microtubule cytoskeletons in prophase, before nuclear envelope breakdown and metaphase (apical view). *Drosophila* embryos expressing the actin-binding domain of moesin fused to GFP were injected with rhodamine-labeled tubulin then either buffer (A) or importin $\alpha$ (B). The actin and microtubule cytoskeletons were followed by time-lapse spinning disk confocal microscopy. (B) Furrows fail to form completely around nuclei leading to the fusion of neighboring spindles (arrows). Arrowhead points to a furrow that surrounds three nuclei. Bars, 10 $\mu$m. (C) Quantitation of the failure in pseudocleavage furrow formation. The number of pseudocleavage furrows observed expressed as a percentage (shown above the column) of the number of furrows expected. Buffer injection, 1203 observed furrows in 20 embryos; Imp $\alpha$ (importin $\alpha$) injection, 1042 furrows observed in 18 embryos; and RanT24N injection, 856 furrows observed in 15 embryos. (D) Distribution of the area of cytoplasm encompassed by furrows around nuclei in cycle 11 embryos. Wild-type embryos (blue), importin $\alpha$–injected embryos (green), and RanT24N-injected embryos (red). (I) small furrows; (II) normal furrows; (III) furrows that surround two nuclei; (IV) furrows that surround three nuclei.

neighboring furrows. Pseudocleavage furrows have four phases of dynamic organization (Figure 3A). In phase I, pseudocleavage furrows ingress at a constant rate for ~4 min to a depth of 10.2 ± 1.45 $\mu$m. The pseudocleavage furrows then remain stationary for 1 min (phase II) before regressing for 4 min (phase III). Finally, the actin cytoskeleton dissipates (phase IV; Figure 3A, Video 2). The simultaneous visualization of pseudocleavage furrows and microtubules showed that phase I occurred during prophase, whereas the end of phase I, phase II, and the beginning of phase III occurred during prometaphase. During metaphase, the pseudocleavage furrow continued to retract (phase III), and by anaphase the furrow was dissipating (phase IV).

Perturbation of the Ran pathway reduced the maximum depth of pseudocleavage furrow ingression from 10.2 ± 1.45 $\mu$m (n = 69) in control embryos to 7.12 ± 1.79 $\mu$m (n = 42, p = 0.0001) in importin $\alpha$–injected embryos (Figure 3A). In addition, perturbation of the Ran pathway disrupted the dynamics of pseudocleavage furrow ingression (Figure 3A). The rate for pseudocleavage furrow ingression during phase I was slower, although it lasted for the same time. Phase II was longer but phase III was shorter, which led to phase IV, dissipation, occurring earlier. As a result pseudocleavage furrows in Ran pathway perturbed embryos had a reduced lifetime. These data suggest that the pseudocleavage furrows that form are disrupted when the Ran pathway is perturbed.

### *Ran Can Regulate Pseudocleavage Furrow Formation Independently of Microtubules*

The Ran pathway is required for organizing the mitotic microtubule cytoskeleton (Ciciarello *et al.*, 2007). In turn these microtubules are required for cytokinetic furrow ingression in somatic cells. However, in *Drosophila* embryos pseudocleavage furrow ingression only requires an intact microtubule cytoskeleton during the anaphase immediately before the ingression of the furrow (Riggs *et al.*, 2007). In contrast, pseudocleavage furrow formation still occurs upon depolymerization of the microtubule cytoskeleton in the telophase immediately before pseudocleavage furrow ingression. Likewise depolymerization of the microtubule cytoskeleton in the interphase during the initial stages of furrow ingression does not disrupt pseudocleavage furrow ingression (Riggs *et al.*, 2007). Because

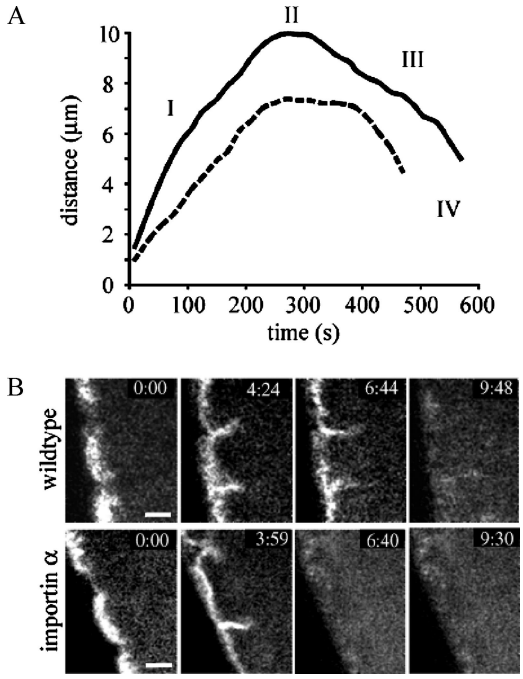


**Figure 3.** Perturbation of the Ran pathway reduces the depth of furrow ingression and reduces the stability of the furrow. (A) Graph of furrow dynamics (in $\mu$m) over time (in seconds) in control embryos (solid line; n = 61 furrows) and embryos injected with importin $\alpha$ (dashed line; n = 42 furrows). The individual curves were averaged, and the averaged plot shows four phases of furrow dynamics: (I) ingression, (II) stable, (III) regression, and (IV) dissipation. (B) Micrographs taken from a time-lapse series of *Drosophila* embryos expressing the actin-binding domain of moesin fused to GFP wild type or injected with importin $\alpha$ (lateral view). Time in minutes: seconds. Bars, 5 $\mu$m.

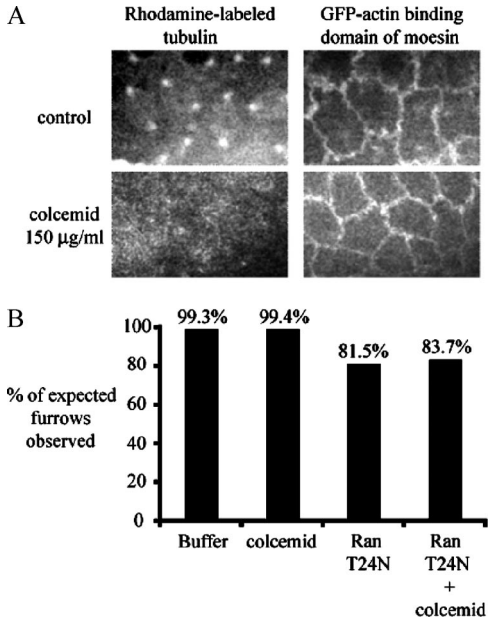


**Figure 4.** Disruption of microtubules during interphase does not disrupt pseudocleavage furrow organization. (A) Embryos expressing GFP fused to the actin-binding domain of moesin were sequentially injected with rhodamine-labeled tubulin in nuclear cycle 10 and then 150 $\mu$g/ml colcemid in interphase of nuclear cycle 11 to depolymerize microtubules. (B) Quantitation of furrow formation in the presence or absence of colcemid and RanT24N. Buffer injection, 1203 observed furrows in 20 embryos; RanT24N injection, 856 furrows observed in 15 embryos; colcemid injection, 452 furrows observed in seven embryos; and RanT24N plus colcemid injection, 320 furrows observed in seven embryos.

we have not observed any defects in interphase microtubule organization upon perturbing the Ran pathway (Figure S1) and because our experimental strategy was to perturb the embryo during interphase (Figure 1), we do not believe that the pseudocleavage furrow defects we observed are due to Ran's disruption of the microtubule cytoskeleton.

To further assess this, we depolymerized microtubules during interphase and observed the subsequent pseudocleavage furrow formation. Embryos expressing GFP fused to the actin-binding domain of moesin were injected during interphase of nuclear cycle 10 with rhodamine-labeled tubulin. Then during interphase of nuclear cycle 11 the embryos were injected with colcemid and pseudocleavage furrow, and microtubule cytoskeleton organization were simultaneously monitored by time-lapse microscopy (Figure 4A). We found that colcemid did not disrupt pseudocleavage furrow formation, because we observed 99.4% of the expected pseudocleavage furrows (Figure 4B), consistent with a previous study (Riggs *et al.*, 2007). However, like the previous study (Riggs *et al.*, 2007), we did see an increase in nuclei surrounded by furrows that encompassed a small area of cytosol (0.8% of nuclei in control embryos compared with 3.2% of nuclei in colcemid injected embryos). We observed a similar increase in this phenotype upon injection of RanT24N (5% of nuclei) and importin $\alpha$ (6.8% of nuclei). This could reflect that this phenotype is due to disruption of the microtubule cytoskeleton, whereas the failure to form a pseudocleavage furrow is not.

Comparing furrow organization in the absence of microtubules (colcemid injection) with furrow organization in the presence of disrupted microtubules (Ran pathway inhibition) may not be optimal, because a misassembled spindle may have stronger negative effects than the lack of a spindle. Therefore we coinjected colcemid with recombinant RanT24N. No increase in the degree of furrow disruption was observed upon the combined injection of RanT24N and colcemid compared with RanT24N alone (Figure 4B). These data suggest that Ran can regulate pseudocleavage furrow formation independently of its role in regulating the mitotic microtubule network.

### *The Ran Pathway Regulates the Recruitment of Peanut to Pseudocleavage Furrows*

To determine how the Ran pathway regulates pseudocleavage furrow ingression, we analyzed the localization of different pseudocleavage furrow components in the presence and absence of Ran pathway inhibitors. Embryos were injected with buffer, RanT24N, or importin $\alpha$ and then fixed and the localization of pseudocleavage furrow components determined by immunofluorescence. All pseudocleavage furrow components tested (diaphanous, cofillin, and myosin regulatory light chain; data not shown) localized to nascent pseudocleavage furrows in embryos injected with importin $\alpha$ or RanT24N, including actin and anillin (Figure 5, A and B). In contrast, the septin Peanut failed to localize to 90% of the nascent pseudocleavage furrows observed (n = 198 furrows in seven embryos) compared with extensive colocalization with actin (data not shown) and anillin in control-injected embryos (Figure 5C). Instead, Peanut had a diffuse localization throughout embryos injected with Ran pathway inhibitors (Figure 5C).

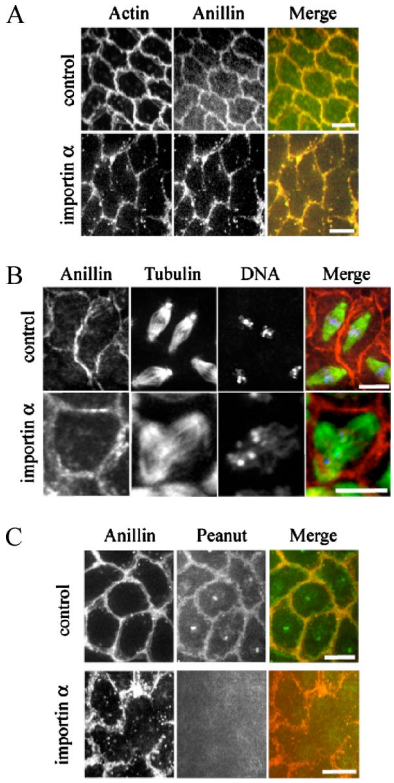


**Figure 5.** Perturbing the Ran pathway prevents the recruitment of Peanut to nascent pseudocleavage furrows. (A) Micrographs of *Drosophila* wild-type embryos or embryos injected with importin α and then fixed and stained with an anti-anillin antibody (green) and rhodamine-labeled phalloidin (red) to detect actin. Colocalization is shown in yellow. (B) Micrographs of *Drosophila* wild-type embryos or embryos injected with importin α and then fixed and stained with an anti-anillin antibody (red), anti-tubulin antibody (green), and DAPI to detect DNA (blue). (C) Micrographs of *Drosophila* embryos wild-type and injected with importin α and then fixed and stained with an anti-anillin antibody (red) and an anti-Peanut antibody (green). Colocalization is shown in yellow. Bars, 10 μm.

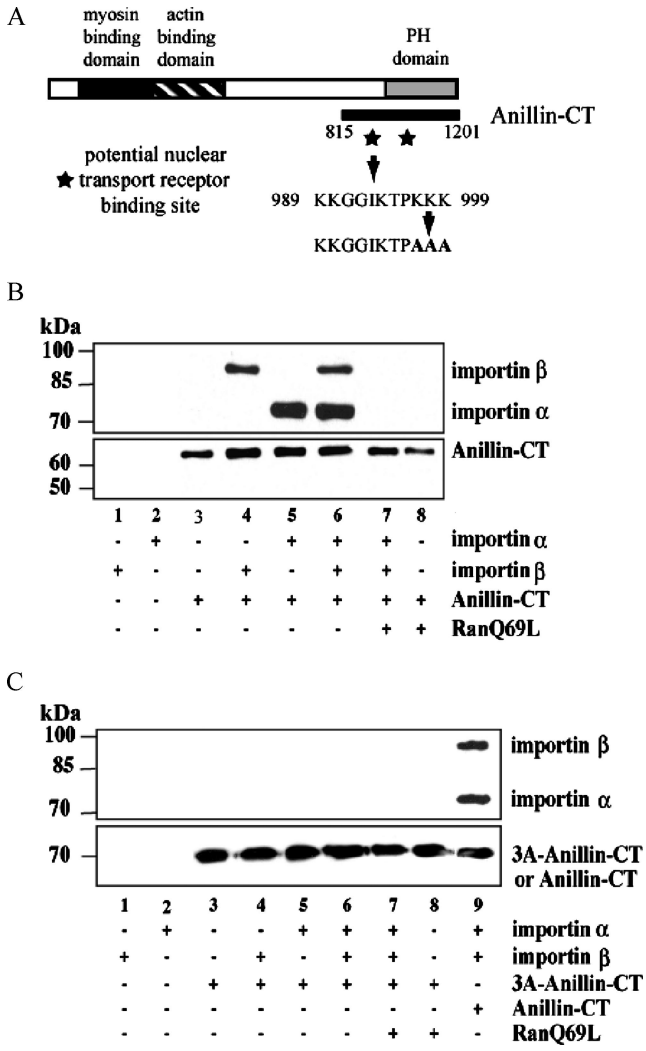


**Figure 6.** Anillin has an importin-binding site adjacent to its PH domain. (A) Diagram outlining the different domains of anillin and the importin-binding site. (B) The carboxy-terminal domain of anillin (amino acids 815-1201, anillin-CT) fused to GST binds to recombinant 6-histidine–tagged importin α and β. Recombinant proteins were mixed and incubated with glutathione agarose beads and then the beads were reisolated. Factors that copurified with the glutathione beads were analyzed by SDS-PAGE and immunoblotted with anti-His tag and anti-GST antibodies. (C) The experiment in B was repeated with a mutated version of the carboxy-terminal domain of anillin where lysines 997–999 were mutated to alanines (3A-anillin-CT).

### *Nuclear Transport Receptors Inhibit Peanut Binding to Anillin*

Peanut is recruited to ingressing furrows by anillin (Field *et al.*, 2005), a multifunctional protein required for cytokinesis that interacts with myosin II, actin, and septins. Septins bind to the carboxy-terminus of anillin, which includes a pleckstrin homology (PH) domain (Oegema *et al.*, 2000; Kinoshita *et al.*, 2002). *Drosophila* anillin has three potential nuclear localization signals (NLS) that could bind to the nuclear transport receptors importin α and β. Two of the NLS motifs are located in or directly adjacent to the PH domain (Oegema *et al.*, 2000; Figure 6A).

To determine if the carboxy-terminus of anillin could bind to importin α and β, we constructed a fusion between GST and the carboxy-terminus of anillin (amino acids 815-1201, anillin-CT, Figure 6A) and analyzed its ability to bind to recombinant importin α and β. Both importin α and β bound to anillin-CT, and this binding was reversed in the presence of RanQ69L, a point mutant of Ran locked in the GTP-bound state (Klebe *et al.*, 1995; Figure 6B). Of the two potential NLS motifs, the one located between amino acid residues 989 and 999, bore the closest resemblance to an archetypal bipartite NLS (Christophe *et al.*, 2000) and is found in the same region of human anillin (amino acids 887–898). Mutation of lysines 997–999 to alanine (3A-anillin-CT) abrogated both importin α and β binding to this region of anillin (Figure 6C), suggesting that amino acids 989–999 constitute a nuclear transport receptor–binding site.

We next asked if the anillin-CT could interact with Peanut. GST-anillin-CT was incubated with 0–3–h *Drosophila* embryo extract and then isolated using glutathione agarose beads. Anillin-CT copurified with Peanut and another septin, Sep2 (Figure 7). However, the addition of exogenous importin α and importin β inhibited the binding of Peanut to anillin-CT in a concentration- and NLS-dependent manner (Figure 7, B and C). This inhibition was specific to Peanut, because Sep2 binding to anillin-CT was not inhibited by importins (Figure 7A).

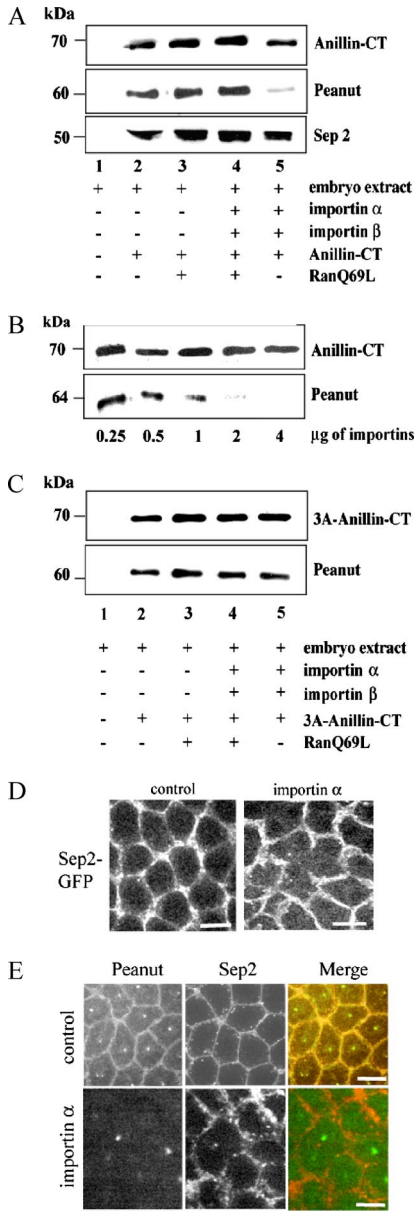


**Figure 7.** Importins inhibit Peanut but not Sep2 binding to anillin and recruitment to pseudocleavage furrows. (A) The carboxy-terminal domain of anillin (amino acids 815-1201, anillin-CT) fused to GST was incubated with *Drosophila* embryo extract in the presence or absence of importin $\alpha$ and $\beta$ and then reisolated using glutathione agarose beads. Copurifying factors were analyzed by SDS-PAGE and Western blotting using antibodies that recognize Peanut and Sep2 and an anti-GST antibody to detect the anillin-CT. (B) GST-anillin-CT was incubated with *Drosophila* embryo extract and increasing amounts of importin $\alpha$ and $\beta$. GST-anillin-CT was reisolated using glutathione agarose beads, and copurifying factors were analyzed by SDS-PAGE and Western blotting to detect Peanut. (C) GST-3A-anillin-CT (GST-anillin-CT with lysine residues 997–999 mutated to alanines) was incubated with *Drosophila* embryo extract in the presence or absence of nuclear transport receptors importin $\alpha$ and $\beta$ and then reisolated using glutathione agarose beads. Copurifying factors were analyzed by SDS-PAGE and Western blotting using antibodies that specifically recognize Peanut and an anti-GST antibody to detect the anillin carboxy-terminal domain. (D) Single time-point micrographs taken from a time-lapse series of GFP-Sep2–expressing embryos that were injected with importin $\alpha$. (E) Micrograph of a wild-type *Drosophila* embryo and one injected with importin $\alpha$ and then fixed and stained with antibodies that recognize Peanut (green) and Sep2 (red). Colocalization in yellow. Bars, 10 $\mu$m.

To determine if the in vivo targeting of Peanut and Sep2 to the pseudocleavage furrows was differentially regulated, importin $\alpha$ was injected into syncytial embryos and GFP-Sep2 localization was determined by time-lapse microscopy. Consistent with our in vitro results, GFP-Sep2 localization was not perturbed upon interfering with the Ran pathway (Figure 7D). Furthermore, in fixed GFP-Sep2–expressing embryos in which the Ran pathway had been perturbed, Peanut failed to localize to nascent furrows, whereas GFP-Sep2 did localize to nascent furrows (Figure 7D). These data suggest that Peanut and Sep2 are differentially regulated by Ran and that Sep2 can localize to pseudocleavage furrows independently of Peanut.

### *Ran Regulates Pseudocleavage Furrow Stability through Anillin and Peanut*

Because anillin and Peanut are required for the stability of the cellularization furrow in *Drosophila* embryos (Field *et al.*, 2005), we sought to determine if Ran regulated pseudocleavage furrow stability by regulating the recruitment of Peanut to pseudocleavage furrows. We generated transgenic *Drosophila* expressing either wild-type GFP-anillin or a mutant anillin, GFP-3A-anillin in which the carboxy-terminal importin binding site we identified had been removed. We hypothesized that by removing the importin binding site from anillin, we should observe a suppression of pseudocleavage furrow defects. Both GFP-tagged anillin constructs localized to furrows as previously observed for wild-type protein (Figures 5 and 8). On injection of recombinant importin $\alpha$ into GFP-anillin expressing embryos, Peanut failed to localize to pseudocleavage furrows (Figure 8A). Similar results were seen upon injection of RanT24N (data not shown). In contrast, injection of importin $\alpha$ into embryos expressing GFP-3A-anillin did not block Peanut recruitment to pseudocleavage furrows. These in vivo findings are consistent with our in vitro data showing that 3A-anillin can still interact with Peanut even in the presence of exogenously added importins.

To address whether Ran-mediated regulation of anillin had a role in pseudocleavage furrow formation and ingression, we also analyzed the effect of inhibiting the Ran pathway in GFP-3A-anillin embryos. First we analyzed the effect of importin $\alpha$ injection on furrow formation in both GFP-anillin and GFP-3A-anillin embryos. We observed 82.5% of the expected pseudocleavage furrows in GFP-anillin embryos where the Ran pathway was perturbed by the injection of importin $\alpha$ (Figure 8B). In contrast, we observed 88.8% of expected pseudocleavage furrows in GFP-3A-anillin embryos. These data suggest that the mutant form of anillin that lacks an importin-binding site cannot fully suppress the furrow formation phenotype, suggesting that Ran may regulate additional factors involved in furrow formation.

Next we analyzed pseudocleavage furrow ingression dynamics upon perturbation of the Ran pathway in both GFP-anillin and GFP-3A-anillin embryos. In embryos expressing GFP-anillin where the Ran pathway was perturbed by injection of importin $\alpha$, pseudocleavage furrows did not ingress as deeply into the embryo (8.14 $\pm$ 0.47 $\mu$m, $p = 0.0084$) as did unperturbed embryos (9.7 $\pm$ 0.63 $\mu$m). In addition, furrows began to regress earlier in Ran pathway–perturbed embryos (Figure 8C). In contrast, in GFP-3A-anillin embryos perturbation of the Ran pathway by injection of importin $\alpha$ did not disrupt the depth of pseudocleavage furrow ingression into the embryo nor the dynamics of pseudocleavage furrow ingression (Figure 8C). These data suggest that Ran through importins regulates Peanut recruitment to

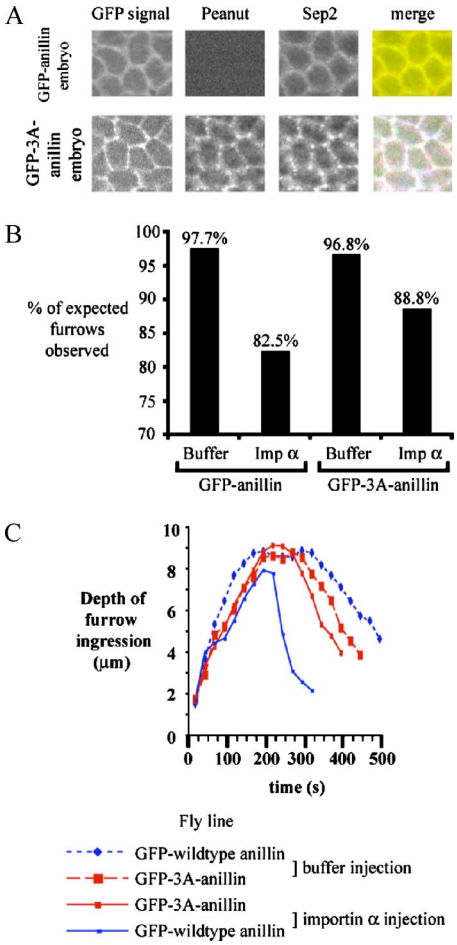


**Figure 8.** Expression of an anillin mutant, 3A-anillin, which lacks an importin-binding site, reverses importin α–mediated inhibition of Peanut recruitment to furrows and importin α induced misregulation of furrow dynamics. (A) GFP-wild-type anillin and GFP-3A-anillin–expressing embryos (both green in the merge panel) were injected with recombinant importin α and then fixed and immunostained to visualize the localization of the septins Peanut (blue in merge) and Sep2 (red in merge). Colocalization of GFP signal and Sep2 is seen as yellow, and colocalization of all three markers appears as white. (B) Quantitation of the failure in pseudocleavage furrow formation. The number of pseudocleavage furrows observed expressed as a percentage (shown above each column) of the number of pseudocleavage furrows expected to form. Buffer injection in GFP-anillin–expressing embryos, 693 furrows observed in seven embryos; importin α injection into GFP-anillin–expressing embryos, 280 furrows observed in five embryos; buffer injection into GFP-3A-anillin–expressing embryos 480 furrows observed in six embryos; and importin α injection into GFP-3A-anillin–expressing embryos, 430 furrows observed in seven embryos. (C) *Drosophila* embryos expressing GFP-wild-type anillin or GFP-3A-anillin were injected with recombinant importin α, and then furrow dynamics were observed.

pseudocleavage furrows and that Peanut recruitment to pseudocleavage furrows promotes furrow stability and ingression to the correct depth in the embryo.

## DISCUSSION

We have identified RanGTP as a regulator of the interaction between Peanut and anillin. This mechanism operates directly and independently of Ran's well-characterized role in regulating the mitotic microtubule cytoskeleton (Ciciarello *et al.*, 2007).

### *Regulation of Septin-Anillin Interaction*

Studies suggest that anillin is required for the recruitment of septins to the furrow (Oegema *et al.*, 2000; Kinoshita *et al.*, 2002; Field *et al.*, 2005). By perturbing the Ran pathway, we demonstrate that the recruitment of the septins Peanut and Sep2 is differentially regulated, consistent with previous observations that Sep1 recruitment to furrows was dependent on Peanut but Sep2 was not (Adam *et al.*, 2000). Anillin lacking the importin binding site between residues 997 and 999 can bind to Peanut in the presence of importins, suggesting that importins directly block the anillin-Peanut interaction rather than disrupting the Peanut, Sep1, and Sep2 complex (Field *et al.*, 1996). These data suggest that although Peanut, Sep1, and Sep2 can exist in a single complex (Field *et al.*, 1996), they may be able to function independently of one another as has been demonstrated in vitro for a *Xenopus* septin (Mendoza *et al.*, 2002).

Perturbing the Ran pathway destabilized pseudocleavage furrows. One mechanism for this is through the regulation of the anillin-Peanut interaction. In embryos that expressed an anillin mutant lacking the importin-binding site, Peanut recruitment to pseudocleavage furrows occurred even in the presence of exogenous importins, and furrows demonstrated wild-type dynamics. These data suggest that Peanut is required for pseudocleavage furrow stability. This role for anillin and Peanut is consistent with the observed role for these proteins in stabilizing the cellularization furrow later in *Drosophila* development (Adam *et al.*, 2000; Field *et al.*, 2005). Our findings may at first appear to contradict those studies in which embryos lacking Peanut protein progressed through the syncytial nuclear divisions only showing the first defects during cellularization (Adam *et al.*, 2000). However, these studies only analyzed syncytial furrows from the top, apical view and not from the lateral view to observe ingression dynamics. Therefore, these studies would not have detected changes in furrow ingression dynamics that we observed upon inhibition of Ran, which correlated with a failure to recruit Peanut to the furrow.

The Ran pathway regulates pseudocleavage furrow ingression directly by regulating importin binding to anillin. We have previously shown that in *Drosophila* syncytial embryos the importin β, whose injection causes similar effects as importin α (Silverman-Gavrila and Wilde, 2006), is released from the nucleus upon nuclear envelope breakdown and becomes diffuse throughout the cytosol during the rest of mitosis (Trieselmann and Wilde, 2002). During this period pseudocleavage furrows begin to retract. Therefore, as importin β is cytosolic during metaphase and anaphase it could act to prevent the interaction of Peanut and anillin. In turn this would lead to furrow instability and retraction.

We cannot unequivocally rule out that some of the defects caused by perturbing the Ran pathway are due to a disruption of microtubule cytoskeleton. Indeed we observed one microtubule-dependent furrow phenotype, the formation of pseudocleavage furrows that encompassed a small area of cytosol around a nucleus. This phenotype was also seen in another study upon depolymerization of microtubules in embryos (Riggs *et al.*, 2007). However, microtubule depolymerization when instigated in interphase does not cause a failure in pseudocleavage furrow formation, a finding consistent with a previous study (Riggs *et al.*, 2007).

Another mechanism through which Ran could affect pseudocleavage furrows is by disrupting nuclear trafficking. Indeed we observe that nuclear trafficking can be reduced by

up to 50% upon disruption of the Ran pathway (Figure S2). However, it seems unlikely that the changes in nuclear import kinetics in our experiments disrupted the function of anillin because anillin is a cytosolic protein in the syncytial embryo and localizes to the leading edge of the ingressing furrow during interphase. It is not understood how anillin is retained in the cytoplasm of syncytial embryos because it is imported into nuclei in other developmental stages. However, this phenomenon is not unique to anillin and is also exhibited by the kinesin Pavarotti, another protein involved in pseudocleavage furrow organization (Minestrini *et al.*, 2003).

### *Implications for Cytokinesis*

Our studies suggest that Ran regulates multiple factors involved in pseudocleavage furrow ingression, because embryos expressing the mutant anillin still exhibit a failure to form all the expected pseudocleavage furrows. Failure to fully suppress the phenotype could be due to the continued presence of endogenous anillin or reflect that other Ran pathway–sensitive factors are involved in pseudocleavage furrow formation. Regulation through the Ran pathway could define a spatial cue concentrated around chromosomes and extending to the cortex. Such a spatiotemporal regulatory mechanism could be involved in promoting cytokinetic furrows in other cells. A recent study in oocytes finds that Ran regulates myosin II (Deng *et al.*, 2007), whose activity is required for cytokinetic cleavage furrows. In addition importin $\alpha$ is required for ring canal organization during oogenesis (Gorjanacz *et al.*, 2002). Ring canals form as a result of incomplete cytokinesis, and many proteins involved in cytokinesis both localize to and are required for their formation, including anillin and septins (Hime *et al.*, 1996).

Our data suggest that the anillin-Peanut interaction, which is inhibited by importins must occur in regions of the cell where there are low levels of importins or high levels of RanGTP. Recent studies have visualized a RanGTP-importin $\beta$ gradient and found that it persists from the chromosomes to the centrosomes (Kalab *et al.*, 2006), a distance similar to that between the metaphase plate and the cortex. Thus, RanGTP could play an important role in positioning the plane of cleavage by defining on the cell cortex where furrow proteins interact.

Although there are clear differences between cytokinetic and pseudocleavage furrows, anillin and septins are involved in both. Therefore, our study suggests that Ran could also have a role in regulating cytokinetic furrows. Whether chromosomes play a significant role in cytokinesis remains controversial (Rappaport and Rappaport, 1974; Rappaport, 1991; Zhang and Nicklas, 1996; Baruni *et al.*, 2008). However, studies where nuclei or chromosomes were asymmetrically positioned within a cell showed that furrow ingression coincided with the region of the cell that contained the chromosomes, suggesting that signals from the nucleus and in particular the chromosomes had a role in specifying furrow ingression (Rappaport, 1991; Canman *et al.*, 2003). Similarly, enucleated sea urchin eggs are able to duplicate their centrosomes and generate astral arrays of microtubules, but failed to form stable cleavage furrows (Sluder *et al.*, 1986). Our study proposes a molecular mechanism to explain, at least in part, these observations, suggesting that RanGTP generated around the chromosomes is a diffusible signal that facilitates multiple processes required for furrow formation. Whether RanGTP is required early in cytokinesis to "prime" the cortex for a future ingression or acts directly later during the ingression process is unclear. Testing these hypotheses is not straightforward, as Ran is also required for organizing the mitotic microtubule cytoskeleton, which is required for cytokinesis. Taken together these findings suggest an additional mechanism involved in regulating cytokinesis that is dependent on signals from chromosomes in addition to those stemming from the different organizational states of the mitotic microtubule cytoskeleton.

## ACKNOWLEDGMENTS

We thank D. Kiehart (Duke University) for GFP-moesin *Drosophila* line, U. Tepass (University of Toronto, Canada) for GFP-spaghetti squash *Drosophila* line, C. Field (Harvard University) for anillin antibody, S. Wasserman (University of California, San Diego) for diaphanous antibody, and T. Uemura (Kyoto University, Japan) for cofillin antibody. We thank J. Pringle and W. Trimble for invaluable discussion and B. Lavoie and J. Brill for critical reading of the manuscript. We thank Carol Ann McCormick, A. Karaiskakis, H. Lipshitz, and C. Smibert for assistance with transgenic flies. K.G.H. was supported by National Research Service Award 1 F32 GM19980-01 from the National Institutes of Health while in the laboratories of John Pringle and Mark Peifer. R.S.-G. received a postdoctoral fellowship from the National Sciences and Engineering Research Council of Canada, and A.W. is funded by grants from the National Cancer Institute of Canada, Canadian Fund for Innovation and holds a Canada Research Chair.

## REFERENCES

Adam, J. C., Pringle, J. R., and Peifer, M. (2000). Evidence for functional differentiation among *Drosophila* septins in cytokinesis and cellularization. Mol. Biol. Cell *11*, 3123–3135.

Afshar, K., Stuart, B., and Wasserman, S. A. (2000). Functional analysis of the *Drosophila* diaphanous FH protein in early embryonic development. Development *127*, 1887–1897.

Albertson, R., Riggs, B., and Sullivan, W. (2005). Membrane traffic: a driving force in cytokinesis. Trends Cell Biol. *15*, 92–101.

Baruni, J. K., Munro, E. M., and von Dassow, G. (2008). Cytokinetic furrowing in toroidal, binucleate and anucleate cells in *C. elegans* embryos. J. Cell Sci. *121*, 306–316.

Brownawell, A. M., Holaska, J. M., Macara, I. G., and Paschal, B. M. (2002). The use of permeabilized cell systems to study nuclear transport. Methods Mol. Biol. *189*, 209–229.

Callaini, G., Dallai, R., and Riparbelli, M. G. (1992). Cytochalasin induces spindle fusion in the syncytial blastoderm of the early *Drosophila* embryo. Biol. Cell *74*, 249–1254.

Canman, J. C., Cameron, L. A., Maddox, P. S., Straight, A., Tirnauer, J. S., Mitchison, T. J., Fang, G., Kapoor, T. M., and Salmon, E. D. (2003). Determining the position of the cell division plane. Nature *424*, 1074–1078.

Caudron, M., Bunt, G., Bastiaens, P., and Karsenti, E. (2005). Spatial coordination of spindle assembly by chromosome-mediated signaling gradients. Science *309*, 1373–1376.

Christophe, D., Christophe-Hobertus, C., and Pichon, B. (2000). Nuclear targeting of proteins: how many different signals? Cell Signal. *12*, 337–341.

Ciciarello, M., Mangiacasale, R., and Lavia, P. (2007). Spatial control of mitosis by the GTPase Ran. Cell Mol. Life Sci. *64*, 1891–1914.

D'Avino, P. P., Savoian, M. S., and Glover, D. M. (2005). Cleavage furrow formation and ingression during animal cytokinesis: a microtubule legacy. J. Cell Sci. *118*, 1549–1558.

Deng, M., Suraneni, P., Schultz, R. M., and Li, R. (2007). The Ran GTPase mediates chromatin signaling to control cortical polarity during polar body extrusion in mouse oocytes. Dev. Cell *12*, 301–308.

Eggert, U. S., Field, C. M., and Mitchison, T. J. (2006). Animal cytokinesis: from parts list to mechanisms. Annu. Rev. Biochem. *75*, 543–566.

Ems-McClung, S. C., Zheng, Y., and Walczak, C. E. (2004). Importin alpha/beta and Ran-GTP regulate XCTK2 microtubule binding through a bipartite nuclear localization signal. Mol. Biol. Cell *15*, 46–57.

Fares, H., Peifer, M., and Pringle, J. R. (1995). Localization and possible functions of *Drosophila* septins. Mol. Biol. Cell *6*, 1843–1859.

Field, C. M., al-Awar, O., Rosenblatt, J., Wong, M. L., Alberts, B., and Mitchison, T. J. (1996). A purified *Drosophila* septin complex forms filaments and exhibits GTPase activity. J. Cell Biol. *133*, 605–616.

Field, C. M., and Alberts, B. (1995). Anillin, a contractile ring protein that cycles from the nucleus to the cell cortex. J. Cell Biol. *131*, 165–178.

Field, C. M., Coughlin, M., Doberstein, S., Marty, T., and Sullivan, W. (2005). Characterization of anillin mutants reveals essential roles in septin localization and plasma membrane integrity. Development *132*, 2849–2860.

Foe, B. E., and Alberts, B. M. (1983). Studies of nuclear and cytoplasmic behavior during the five mitotic cycles that precede gastrulation in *Drosophila* embryos. J. Cell Sci. *61*, 31–70.

Glotzer, M. (2001). Animal cell cytokinesis. Ann. Rev. Cell Dev. Biol. *17*, 351–386.

Gorjanacz, M., Adam, G., Torok, I., Mechler, B. M., Szlanka, T., and Kiss, I. (2002). Importin-alpha 2 is critically required for the assembly of ring canals during *Drosophila* oogenesis. Dev. Biol. *251*, 271–282.

Gregory, S. L., Ebrahimi, S., Milverton, J., Jones, W. M., Bejsovec, A., and Saint, R. (2008). Cell division requires a direct link between microtubule-bound RacGAP and Anillin in the contractile ring. Curr. Biol. *18*, 25–29.

Grieder, N. C., deCuevas, M., and Spradling, A. C. (2000). The fusome organizes the microtubule network during oocyte differentiation in *Drosophila.* Development *127*, 4253–4264.

Hickson, G. R., and O'Farrell, P. H. (2008). Rho-dependent control of anillin behavior during cytokinesis. J. Cell Biol. *180*, 285–294.

Hime, G. R., Brill, J. A., and Fuller, M. T. (1996). Assembly of ring canals in the male germ line from structural components of the contractile ring. J. Cell Sci. *109*, 2779–2788.

Hyman, A. A. (1991). Preparation of marked microtubules for the assay of the polarity of microtubule based motors by fluorescence. J. Cell Sci. (Suppl.) *14*, 125–127.

Janetopoulos, C., and Devreotes, P. (2006). Phosphoinositide signaling plays a key role in cytokinesis. J. Cell Biol. *174*, 485–489.

Joo, E., Surka, M. C., and Trimble, W. S. (2007). Mammalian SEPT2 is required for scaffolding nonmuscle myosin II and its kinases. Dev. Cell *13*, 677–690.

Kalab, P., Pralle, A., Isacoff, E. Y., Heald, R., and Weis, K. (2006). Analysis of a RanGTP-regulated gradient in mitotic somatic cells. Nature *440*, 697–701.

Kiehart, D. P., Galbraith, C. G., Edwards, K. A., Rickoll, W. L., and Montague, R. A. (2000). Multiple forces contribute to cell sheet morphogenesis for dorsal closure in *Drosophila.* J. Cell Biol. *149*, 471–490.

Kinoshita, M., Field, C. M., Coughlin, M. L., Straight, A. F., and Mitchison, T. J. (2002). Self- and actin-templated assembly of mammalian septins. Dev. Cell *3*, 791–802.

Klebe, C., Prinz, H., Wittinghofer, A., and Goody, R. S. (1995). The kinetic mechanism of Ran–nucleotide exchange catalyzed by RCC1. Biochemistry *34*, 12543–12552.

Kornbluth, S., Dasso, M., and Newport, J. (1994). Evidence for a dual role for TC4 protein in regulating nuclear structure and cell cycle progression. J. Cell Biol. *125*, 705–719.

Li, H. Y., and Zheng, Y. (2004). Phosphorylation of RCC1 in mitosis is essential for producing a high RanGTP concentration on chromosomes and for spindle assembly in mammalian cells. Genes Dev. *18*, 512–527.

Mazumdar, A., and Mazumdar, M. (2002). How one becomes many: blastoderm cellularization in *Drosophila melanogaster*. Bioessays *24*, 1012–1022.

Mendoza, M., Hyman, A. A., and Glotzer, M. (2002). GTP binding induces filament assembly of a recombinant septin. Curr. Biol. *12*, 1858–1863.

Minestrini, G., Harley, A. S., and Glover, D. M. (2003). Localization of pavarotti-KLP in living *Drosophila* embryos suggests roles in reorganizing the cortical cytoskeleton during the mitotic cycle. Mol. Biol. Cell *14*, 4028–4038.

Nelson, M. R., Leidal, A. M., and Smibert, C. A. (2004). *Drosophila* Cup is an eIF4E-binding protein that functions in Smaug-mediated translational repression. EMBO J. *23*, 150–159.

Neufeld, T. P., and Rubin, G. M. (1994). The *Drosophila* peanut gene is required for cytokinesis and encodes a protein similar to yeast putative bud neck filament proteins. Cell *77*, 371–379.

Niwa, R., Nagata-Ohashi, K., Takeichi, M., Mizuno, K., and Uemura, T. (2002). Control of actin reorganization by Slingshot, a family of phosphatases that dephosphorylate ADF/cofilin. Cell *108*, 233–246.

Oegema, K., Savoian, M. S., Mitchison, T. J., and Field, C. M. (2000). Functional analysis of a human homologue of the *Drosophila* actin binding protein anillin suggests a role in cytokinesis. J. Cell Biol. *150*, 539–552.

Piekny, A. J., and Glotzer, M. (2007). Anillin is a scaffold protein that links RhoA, actin and myosin during cytokinesis. Curr. Biol. *18*, 3–36.

Rappaport, R. (1991). Enhancement of aster-induced furrowing activity by a factor associated with the nucleus. J. Exp. Zool. *257*, 87–95.

Rappaport, R., and Rappaport, B. N. (1974). Establishment of cleavage furrows by the mitotic spindle. J. Exp. Zool. *189*, 189–196.

Riggs, B., Fasulo, B., Royou, A., Mische, S., Cao, J., Hays, T. S., and Sullivan, W. (2007). The concentration of Nuf, a Rab11 effector, at the microtubule-organizing center is cell cycle regulated, dynein-dependent, and coincides with furrow formation. Mol. Biol. Cell *18*, 3313–3322.

Royou, A., Sullivan, W., and Karess, R. (2002). Cortical recruitment of nonmuscle myosin II in early syncytial *Drosophila* embryos: its role in nuclear axial expansion and its regulation by Cdc2 activity. J. Cell Biol. *158*, 127–137.

Rubin, G. M., and Spradling, A. C. (1982). Genetic transformation of *Drosophila* with transposable element vectors. Science *218*, 348–353.

Silverman-Gavrila, R. V., and Wilde, A. (2006). Ran is required before metaphase for spindle assembly and chromosome alignment and after metaphase for chromosome segregation and spindle midbody organization. Mol. Biol. Cell *17*, 2069–2080.

Sluder, G., Miller, F. J., and Rieder, C. L. (1986). The reproduction of centrosomes: nuclear versus cytoplasmic controls. J. Cell Biol. *103*, 1873–1881.

Sullivan, W., Minden, J. S., and Alberts, B. M. (1990). daughterless-abo-like, a *Drosophila* maternal-effect mutation that exhibits abnormal centrosome separation during the late blastoderm divisions. Development *110*, 311–323.

Takizawa, P. A., DeRisi, J. L., Wilhelm, J. E., and Vale, R. D. (2000). Plasma membrane compartmentalization in yeast by messenger RNA transport and a septin diffusion barrier. Science *290*, 341–344.

Thummel, C., and Pirrotta, V. (1992). Technical notes: new pCaSpeR P element vectors. Dros. Inf. Serv. *71*, 150.

Trieselmann, N., Armstrong, S., Rauw, J., and Wilde, A. (2003). Ran modulates spindle assembly by regulating a subset of TPX2 and Kid activities including Aurora A activation. J. Cell Sci. *116*, 4791–4798.

Trieselmann, N., and Wilde, A. (2002). Ran localizes around the microtubule spindle *in vivo* during mitosis in *Drosophila* embryos. Curr. Biol. *12*, 1124–1129.

Warn, R. M., Magrath, R., and Webb, S. (1984). Distribution of F-actin during cleavage of the *Drosophila* syncytial blastoderm. J. Cell Biol. *98*, 156–162.

Zhang, D., and Nicklas, R. B. (1996). "Anaphase" and cytokinesis in the absence of chromosomes. Nature *382*, 466–468.